Proc. Natl. Acad. Sci. USA
Vol. 95, pp. 14687–14692, December 1998
Biochemistry

Double-stranded RNA induces mRNA degradation in *Trypanosoma brucei*

HUÂN NGÔ*, CHRISTIAN TSCHUDI*, KEITH GULL†, AND ELISABETTA ULLU*‡§

Departments of *Internal Medicine and ‡Cell Biology, Yale University School of Medicine, 333 Cedar Street, New Haven, CT 06520-8022; and †School of Biological Sciences, University of Manchester, 2.205 Stopford Building, Oxford Road, Manchester M13 9PT, United Kingdom

Communicated by Joan A. Steitz, Yale University, New Haven CT, October 16, 1998 (received for review September 9, 1998)

ABSTRACT **Double-stranded RNA (dsRNA) recently has been shown to give rise to genetic interference in *Caenorhabditis elegans* and also is likely to be the basis for phenotypic cosuppression in plants in certain instances. While constructing a plasmid vector for transfection of trypanosome cells, we serendipitously discovered that *in vivo* expression of dsRNA of the α-tubulin mRNA 5′ untranslated region (5′ UTR) led to multinucleated cells with striking morphological alterations and a specific block of cytokinesis. Transfection of synthetic α-tubulin 5′ UTR dsRNA, but not of either strand individually, caused the same phenotype. On dsRNA transfection, tubulin mRNA, but not the corresponding pre-mRNA, was rapidly and specifically degraded, leading to a deficit of α-tubulin synthesis. The transfected cells were no longer capable of carrying out cytokinesis and eventually died. Analysis of cytoskeletal structures from these trypanosomes revealed defects in the microtubules of the flagellar axoneme and of the flagellar attachment zone, a complex cortical structure that we propose is essential for establishing the path of the cleavage furrow at cytokinesis. Last, dsRNA-mediated mRNA degradation is not restricted to α-tubulin mRNA but can be applied to other cellular mRNAs, thus establishing a powerful tool to genetically manipulate these important protozoan parasites.**

Over the last 10 years, the study of RNA metabolism in trypanosomatid protozoa has unraveled novel mechanisms of eukaryotic gene expression such as polycistronic transcription (1), trans-splicing (2, 3), mitochondrial RNA editing (4–6), and coupling of trans-splicing and polyadenylation (7). Furthermore, in these organisms, RNA polymerase II promoters have not been identified. So far, regulation of expression of polymerase II genes has been documented only at the post-transcriptional level, with clear evidence that cis-acting mRNA sequences play a role in mRNA stability. However, regulation of pre-mRNA turnover, trans-splicing, polyadenylation, and mRNA export from the nucleus to the cytoplasm likely are additional steps for modulating the output of mature mRNA from a given gene. Notwithstanding our present limited knowledge of these subjects, it appears that trypanosome mRNA abundance is primarily, if not solely, regulated at the level of RNA metabolism rather that at the level of transcription initiation, as is the case in most eukaryotic organisms. How the various steps involved in mRNA metabolism are integrated to generate diversity at the level of mRNA abundance is not known.

We have observed that challenging *Trypanosoma brucei* cells with gene-specific double-stranded RNAs (dsRNAs) leads to specific degradation of the homologous mRNA. We serendipitously discovered this pathway because trypanosomes expressing dsRNA representing a portion of α-tubulin mRNA acquired an abnormal phenotype, namely, they became multinucleated and lost their typical slender morphology. In addition to providing evidence for dsRNA-mediated mRNA degradation in trypanosomes, our analysis uncovered that among the microtubule-mediated processes, cytokinesis is highly sensitive to a decrease in the pool of α-tubulin. The observation that cytokinesis-arrested trypanosomes have alterations of the flagellar axoneme and of the cortical cytoskeleton subtending the flagellum suggests a role for these cytoskeletal elements in cytokinesis.

MATERIALS AND METHODS

RNA Synthesis and Transfection. RNA was synthesized from linear DNA templates by using the Ampliscribe T7 RNA polymerase kit from Epicentre Technologies (Madison, WI). After digestion with DNase I, RNA was purified by using chromatography through a P-6 spin column (Bio-Rad) and analyzed by electrophoresis on a sequencing gel. dsRNA was generated by annealing equimolar amounts of the sense and antisense transcripts in 300 mM NaCl, 50 mM Tris·HCl (pH 7.5), and 1 mM EDTA at 68°C for 1 hr. The RNA was then recovered by ethanol precipitation and resuspended in water. For each transfection, 10^8 procyclic *T. brucei rhodesiense* cells, strain Ytat1.1, were washed four times in Cytomix (120 mM KCl/0.15 mM $CaCl_2$/10 mM K_2HPO_4/25 mM Hepes (pH 7.6)/2 mM EDTA/5 mM $MgCl_2$) and resuspended in 0.5 ml of Cytomix. To minimize the possibility of degradation, dsRNA (1–50 μg per 10^8 cells in 100 μl of water) was added to the cells just before electroporation. Cells were electroporated by using a Bio-Rad Gene Pulser set at 1.5 kV and 25 μF in 0.4-cm-gap cuvettes using two pulses delivered 10 sec apart and immediately transferred into fresh medium. The same conditions were used for DNA transfection, except that 100 μg of plasmid DNA was used per transfection.

Electron Microscopy. For transmission electron microscopy, cells were prepared as described (8), and thin sections were examined in a JEOL microscope. Cells were processed for scanning electron microscopy at the Cell Imaging Center at the Marine Biological Laboratory in Woods Hole, MA.

Immunofluorescence. Cells were washed in PBS, settled on poly-L-lysine-coated slides, and fixed in −20°C methanol for 20 min. Cells were incubated in PBS with 10% fetal bovine serum for 30 min and in the same solution containing the primary antibody for 1 hr. After washing with PBS, cells were reacted with a fluorescein isothiocyanate (FITC)- or rhodamine-conjugated secondary antibody, washed again, and mounted in FluorSave Reagent medium (Calbiochem) containing 0.5 μg/ml 4′,6-diamidino-2-phenylindole (DAPI). For visualizing green fluorescent protein (GFP), cells were fixed on ice in 2%

The publication costs of this article were defrayed in part by page charge payment. This article must therefore be hereby marked "*advertisement*" in accordance with 18 U.S.C. §1734 solely to indicate this fact.

Abbreviations: DAPI, 4′,6-diamidino-2-phenylindole; dsRNA, double-stranded RNA; GFP, green fluorescent protein; PFR, paraflagellar rod; 5′ UTR, 5′ untranslated region.

§To whom reprint requests should be addressed. e-mail: elisabetta.ullu@yale.edu.

paraformaldehyde for 20 min, washed, and incubated for 1–2 min in PBS containing 0.01% saponin and 0.5 μg/ml DAPI, washed again, and mounted in the above medium. Cells were imaged by using a Nikon Microphot-FXA microscope, and images were captured with the Photometrix Sensys charge-coupled device camera by using the PHASE3 IMAGE software.

RESULTS

Transient Expression or Electroporation of α-Tubulin dsRNA Induces the Appearance of Multinucleated Cells. We made the serendipitous observation that transient expression of plasmid pGFPFAT (Fig. 1) in cultured insect forms (procyclic) of *T. brucei rhodesiense* (Fig. 2*a*) led to cells with an altered morphology and multiple nuclei and kinetoplasts (mitochondrial DNA). Scanning electron microscopy (Fig. 2*b*) revealed that the transfected cells were almost spherical, with pronounced ruffling of the surface. We named these cells FAT cells. These initial observations suggested that expression of pGFPFAT was interfering with cytokinesis and with the cytoskeletal organization of trypanosome cells.

To identify the sequences responsible for the FAT cell phenotype, several derivatives of pGFPFAT were constructed (Fig. 1) and transfected into trypanosomes. Of note in the structure of pGFPFAT is the presence of two complete copies of the α-tubulin mRNA 5′ untranslated region (UTR) of 113 nucleotides (9) in a head-to-head configuration and separated by a 700-nt sequence unrelated to α-tubulin. Because the FAT phenotype was lost when the promoter was eliminated (pGFPFATΔP) and whenever either of the two α-tubulin 5′ UTRs was removed (pFATΔBX and pFATΔUP1), we predicted that the active molecule was a transcript extending through the two α-tubulin 5′ UTRs, probably in the form of a long dsRNA stem with a single-stranded loop. Indeed, a transcript of the predicted size was detected by Northern blot hybridization (data not shown).

To test our hypothesis, we transfected procyclic trypanosomes with RNA made *in vitro* with T7 RNA polymerase. RNA extending from one α-tubulin 5′ UTR to the other (RNA1 in Fig. 1) induced the FAT phenotype. Next, we separately synthesized sense and antisense transcripts of the α-tubulin 5′ UTR. Production of FAT cells was seen only when the two transcripts were annealed before electroporation (FAT RNA in Fig. 1). As controls for the specificity of this effect, we used an unrelated dsRNA sequence of similar length to the α-tubulin 5′ UTR and commercially available poly(I)·poly(C), which is the common inducer for dsRNA-activated protein kinase. Neither of these two RNAs had any detectable effect on electroporation into trypanosome cells. We found that the percentage of FAT cells increased linearly with the amount of transfected FAT RNA until most of the cells acquired the FAT phenotype (Fig. 2*c*).

dsRNA Induces mRNA Degradation. To begin an analysis of the molecular mechanism underlying the establishment of the FAT cell phenotype, we determined the fate of α-tubulin mRNA in cells transfected with the FAT RNA by using Northern blotting and phosphorimager analysis (Fig. 3*a*). Relative to control RNA (time 0), there was about an 85% reduction in the amount of α-tubulin mRNA in FAT cells as early as 1 hr after transfection. α-Tubulin mRNA levels stayed low up to 10 hr after transfection but after 20 hr returned to about 50% of the α-tubulin mRNA level present in control RNA. Within 1 hr of transfection, β-tubulin mRNA decreased to about 1/2 that of control cells, but mRNA levels rapidly returned to normal. Perhaps the reduction of β-tubulin mRNA in FAT RNA-transfected cells resulted from the need to coordinate regulation of α- and β-tubulin synthesis, but we have not investigated this phenomenon further. In contrast, mRNAs coding for the trypanosome homologue of the human autoantigen La (GenBank accession no. AA003497) and for

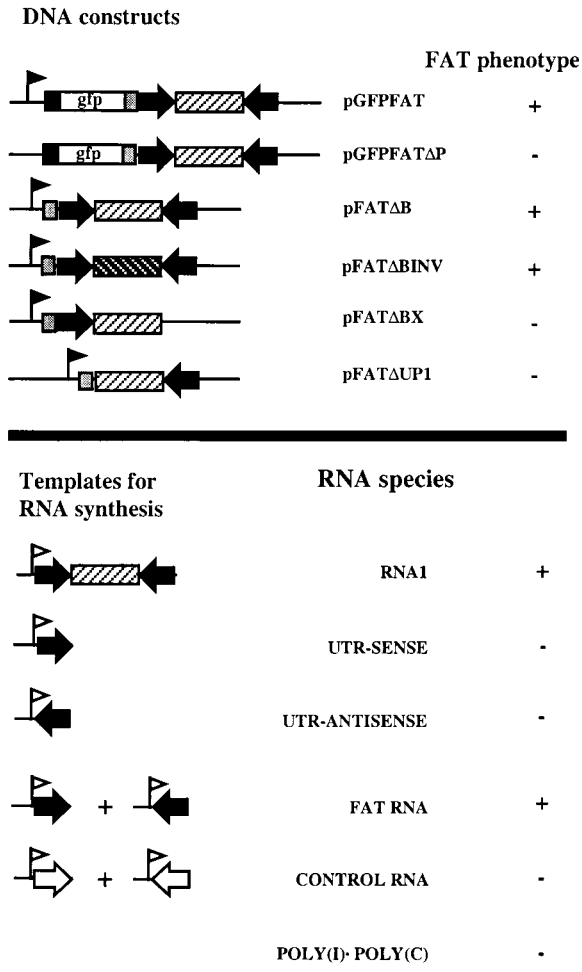

FIG. 1. DNA constructs and RNA species used to analyze dsRNA effects. pGFPFAT DNA contains in a 5′- to-3′ direction the following components: the ribosomal promoter (solid flag), sequences from the nucleotide after the termination codon of β-tubulin to the nucleotide preceding the initiation codon of α-tubulin (solid box), the GFP coding region (gfp), the 3′ UTR and poly(A) site region of the procyclic acidic repetitive protein gene (ref. 7; shaded box), the α-tubulin 5′ UTR in the sense orientation (solid arrow), a portion of the spliced leader RNA gene repeat from nucleotide 999 of one repeat unit to nucleotide 346 of the adjacent repeat unit (ref. 22; hatched box), and the α-tubulin 5′ UTR in the antisense configuration (solid arrow). In pFATΔBINV, the spliced leader gene sequence (dark-hatched box) was present in the opposite orientation as compared with pGFPFAT DNA. All of the sequences, except for the GFP gene, were derived from *T. brucei* DNA. All templates for RNA synthesis contained the T7 RNA polymerase promoter (open flag) located about 10 nucleotides upstream from the transcription initiation site. Control RNA transcripts were derived from transcription of templates containing synthetic sequences (open arrows) of identical length to the α-tubulin 5′ UTR, and which were generated from the α-tubulin 5′ UTR sequence by changing each A residue to a C residue, each G residue to a T residue, and vice versa. The sense or antisense configuration of each transcript is indicated by the direction of the arrow relative to the promoter.

the paraflagellar rod (PFR) A protein (10) as well as the mRNA for a chromosomally integrated copy of a GFP transgene (data not shown) remained constant during the same time period. We found that the FAT cell phenotype could also be elicited by dsRNA derived from nucleotides 670–784 of the α-tubulin coding sequence as well as by dsRNA of the β-tubulin mRNA 5′ UTR, which is only 59 nucleotides long (data not shown). In both instances, the kinetics of degradation of the respective mRNAs were similar to the one shown in Fig. 3*a*.

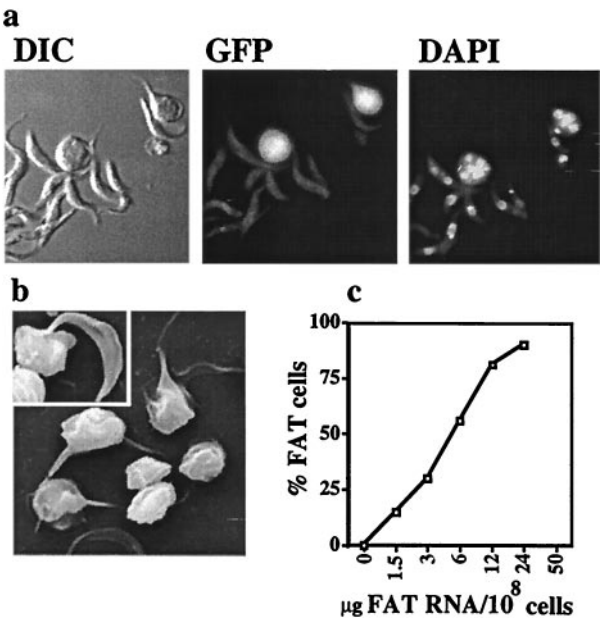

FIG. 2. Transient expression of dsRNA representing the α-tubulin mRNA 5′ UTR induces the appearance of trypanosomes with the FAT phenotype. (*a*) Cell types after transient expression of pGFPFAT DNA in cultured insect form trypanosomes. Twenty hours after transfection, cells were fixed, permeabilized, and stained with the DNA intercalating dye DAPI. Cells were visualized with a 60× Nikon lens by differential interference contrast. GFP expression was detected by illumination with a fluorescein isothiocyanate filter. (*b*) Scanning electron micrographs of trypanosome cells expressing pGFPFAT DNA. Thirty-six hours after transfection, FAT cells were harvested by centrifugation, deposited on glass coverslips, fixed, and processed for scanning electron microscopy. Magnification was ×1,400. The *Inset* shows the appearance of a normal procyclic trypanosome cell. (*c*) Percentage of FAT cells as a function of the amount of electroporated synthetic FAT RNA.

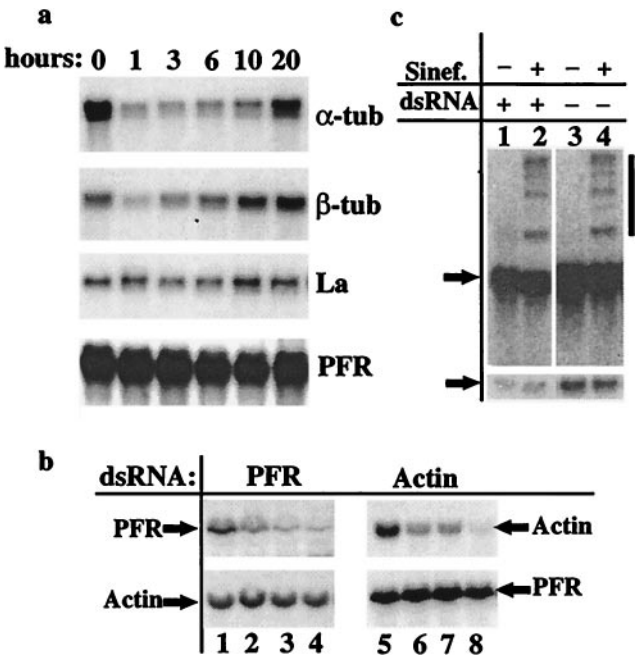

FIG. 3. Effects of various dsRNAs on levels of endogenous RNA transcripts. (*a*) Cells were electroporated with FAT RNA (10 μg per 10^8 cells), and total RNA was extracted at the times indicated above the lanes. Following fractionation on a 1.2% agarose/2.2 M formaldehyde gel, mRNAs were visualized by using Northern blotting and hybridization to gene-specific probes as indicated in the figure. (*b*) Different amounts of PFR dsRNA (nucleotides 1–465 of the protein-coding region) or actin ds-RNA (nucleotides 1–446 of the protein-coding region) were electroporated into cells, and total RNA was extracted 3 hr later. Duplicate blots were hybridized with gene-specific probes as indicated in the figure. In lanes 1 and 5, cells were electroporated with 10 μg of poly(I)·poly(C). The remainder of the lanes received the following amounts of the corresponding dsRNAs: 2 μg of dsRNA (lanes 2 and 6), 4 μg of dsRNA (lanes 3 and 7), and 10 μg of dsRNA (lanes 4 and 8). (*c*) Cells were electroporated with FAT RNA (lanes 1 and 2; 10 μg per 10^8 cells) or with poly(I)·poly(C) (lanes 3 and 4; 10 μg per 10^8 cells), and half of the cells in each sample received 2 μg/ml sinefungin (lanes 2 and 4). After a 90-min incubation, total RNA was extracted, processed for Northern blotting, and hybridized to an antisense α-tubulin coding region probe. Arrows indicate α-tubulin mRNA. The bar indicates the position of polycistronic tubulin RNAs. A long (*Upper*) and a short (*Lower*) exposure of the same autoradiogram are shown. Sinefungin inhibition of methylation of the spliced leader RNA cap structure (12), and thus inhibition of trans-splicing (23), was verified by using primer-extension analysis of the spliced leader RNA at different times after addition of the drug (data not shown). As reported previously (12), maximal inhibition was observed after 30 min. Cells remained actively motile throughout the duration of the experiment.

Next, we asked whether other trypanosome mRNAs could be targeted for degradation by dsRNAs. Fig. 3*b* shows that both actin and PFR mRNAs were specifically degraded by transfection of corresponding dsRNAs of about 450 nucleotides. Although we have not systematically analyzed the length requirements for dsRNA-mediated mRNA degradation, we have found that increasing the length of actin and PFR dsRNAs from 100 to 450 nucleotides resulted in a significant increase in the degradation of the corresponding mRNAs (data not shown).

To begin to understand the mechanism of dsRNA-mediated mRNA degradation, we asked whether the FAT RNA was targeting for destruction the mature α-tubulin mRNA, the tubulin pre-mRNA, or both. To this end, we took advantage of the observation that inhibition of trans-splicing leads to accumulation of polycistronic pre-mRNA in *T. brucei* (11). Immediately after transfection with the FAT RNA, we blocked trans-splicing with sinefungin (a methylation inhibitor that prevents modification of the spliced leader RNA cap 4 structure, ref. 12) and assessed by using Northern blotting the accumulation of polycistronic tubulin pre-mRNA during a 90-min incubation period. The results of this analysis (Fig. 3*c*) showed that the amount of tubulin polycistronic pre-mRNAs in sinefungin-treated FAT cells was indistinguishable from that present in sinefungin-treated control cells. Because the half-life of α-tubulin mRNA is longer than 90 min (E.U., unpublished observations), this result argued that the target of FAT RNA-mediated degradation was predominantly the mature α-tubulin mRNA.

Transient Knockout of Tubulin Synthesis Blocks Cytokinesis. The reduction of α-tubulin mRNA levels observed 1 hr after transfection of FAT RNA (Fig. 3*a*) resulted in about 80% inhibition of α-tubulin synthesis as determined by a 30-min pulse with ^{35}S-labeled amino acids and quantitation of radiolabeled α-tubulin from two-dimensional gels (Table 1). However, in agreement with the results of the Northern blot reproduced in Fig. 3*a*, the synthesis of α-tubulin returned to about control levels 16 hr after transfection. By two-dimensional gel analysis we did not detect any other anomaly in the pattern of ^{35}S-labeled proteins (data not shown). Thus, electroporation of FAT RNA induced a specific but only transient knockout of α-tubulin synthesis, probably because the FAT RNA was degraded within cells. On the other hand, FAT cells were permanently damaged in their ability to carry out cytokinesis and after a few days in culture, formed macroscopic aggregates and died.

To document cytologically the cytokinesis block, we determined the time course of FAT cell appearance by following the

Table 1. Tubulin synthesis in FAT cells

	Synthesis, %			
	1 hr		16 hr	
Tubulin	FAT	Control	FAT	Control
α-Tubulin	22	100	90	100
β-Tubulin	70	100	83	100

Trypanosome cells were electroporated with FAT RNA or poly(I)·poly(C) as a control, and 1 hr or 16 hr after transfection, were pulsed for 30 min with ^{35}S-radiolabeled amino acids. Radiolabeled proteins were separated by two-dimensional gels, and the positions of α- and β-tubulin were determined by using Western blot analysis with specific mAbs. The levels of radioactivity associated with α- and β-tubulin were determined by PhosphorImager analysis and are expressed as percentages of α- and β-tubulin synthesized in control cells, which are set at 100.

accumulation of cells with more than one nucleus and kinetoplast. Cells with one kinetoplast and one nucleus (1K1N) are early in the cell cycle, cells with two kinetoplasts and one nucleus (2K1N) have segregated the kinetoplasts and are positioned later in the cell cycle, and cells with two kinetoplasts and two nuclei (2K2N), have completed mitosis and are poised for cytokinesis (13). As shown in Table 2, at time 0 the majority of cells were 1K1N or 2K1N, with only about 4% of cells being 2K2N, as expected for an asynchronously growing trypanosome cell population. Between 4 and 10 hr posttransfection (which, for our cells, corresponds to approximately the duration of one cell cycle), the number of 2K2N cells increased to about 30%, with a concomitant decrease in 1K1N and 2K1N cells. At 20 hr posttransfection—after about two cell cycles—a new population of cells with four nuclei became prevalent. These 4N cells were most likely derived by a second cycle of mitotic division from 2K2N cells. However, it was not possible to determine with certainty the number of kinetoplasts in the 4N cells because of their complex three-dimensional geometry. Cells at 0, 8, and 20 hr posttransfection also were processed for immunofluorescence and decorated with mAb YL 1/2 that recognizes only tyrosinated α-tubulin, namely, α-tubulin that has been recently added to the microtubule ends (14) and ROD-1 (15) that recognizes the PFR of the trypanosome flagellum (Fig. 4). From these images, it was evident that the morphology of 8-hr FAT cells was already altered relative to that of cells at time 0. Within this cell population, the 2K2N cells had successfully segregated the basal bodies, which are strongly stained by YL 1/2, and had duplicated their flagella. Thus, these cells had progressed through the cell cycle but were arrested before cytokinesis.

The cytoskeletal elements of FAT cells 20 hr posttransfection also were examined by electron microscopic studies (Fig. 5), which did not reveal any morphological defects of the basal bodies or any detectable discontinuities in the corset of cortical microtubules subtending the plasma membrane. However, in at least one of the flagella of a FAT cell, the central pair and several outer doublet microtubules of the axoneme were not

Table 2. Proportions of trypanosome cell types as a function of time after transfection with FAT RNA

Cell type	0 hr	3.5 hr	6.5 hr	10 hr	20 hr
1K1N	84	85	79	64	22
2K1N	12	12	5	5	—
2K2N	4	3	16	31	32
4N	—	—	—	—	46

Cells were transfected with FAT RNA (10 μg per 10^8 cells), and aliquots were fixed and stained with DAPI at the indicated times. For each time point, 150 cells were analyzed. The percentage of each cell type is indicated. 1K1N, one kinetoplast and one nucleus; 2K1N, two kinetoplasts and one nucleus; 2K2N, two kinetoplasts and two nuclei; 4N, four nuclei.

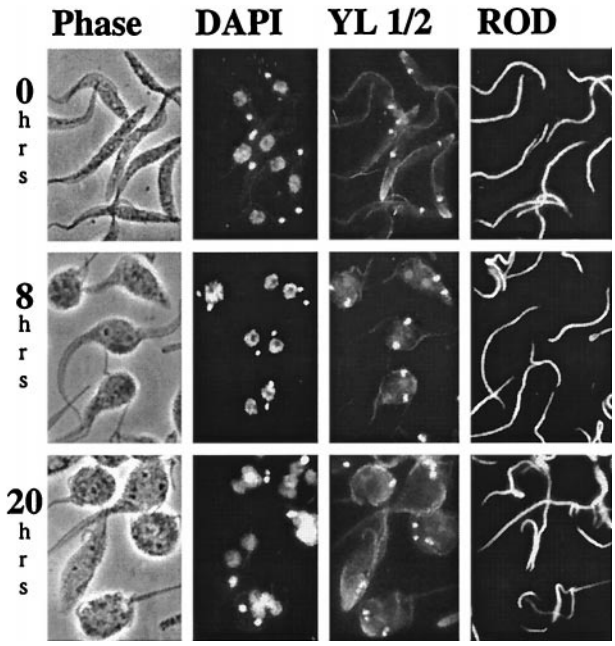

FIG. 4. Effects of FAT RNA on various trypanosome organelles. Cells were transfected with FAT RNA and processed for indirect immunofluorescence at the indicated times. Nuclei and kinetoplasts were stained with DAPI, tyrosinated α-tubulin was decorated with rat mAb YL 1/2 (14) and fluorescein isothiocyanate-conjugated anti-rat IgG secondary antibody (panels YL 1/2), and the PFR of the flagellum was immunostained with mouse mAb ROD-1 (15) and a rhodamine-conjugated anti-mouse IgG secondary antibody (ROD panels). In the DAPI images, kinetoplast DNA appears as discrete dots. The bright-stained dots in the YL 1/2 images are basal bodies. Images were obtained with a 100× PlanApo/1.4 Nikon lens.

assembled. Most likely these abnormal axonemes were not properly assembled when soluble α-tubulin was limiting. We observed also that an abnormal flagellar axoneme was spatially linked to another cytoskeletal defect, namely the lack of one or more microtubules of a specific quartet of cortical microtubules that is located immediately left of the flagellum when viewed from the posterior end of the cell. These four microtubules are differentiated from the remaining cortical microtubules by their close association to smooth endoplasmic reticulum, their stability to salt dissociation, and their association with γ-tubulin and are part of the flagellar attachment zone, the filament system that connects the flagellum to the cortical array of microtubules (16). In a small proportion of the FAT cells, some of the cortical microtubules on either side of the flagellar attachment zone also were found to be absent.

DISCUSSION

dsRNA-mediated mRNA degradation in trypanosomes adds to the list of biological activities that recently have been attributed to dsRNA molecules, most notably the powerful genetic interference elicited by dsRNA microinjected into the nematode *Caenorhabditis elegans* (17). In this case, although direct evidence is lacking, it has been hypothesized that dsRNA may result in early degradation of the endogenous mRNA (17). RNA-dependent mRNA degradation, possibly via formation of dsRNA, also has been described in plants, where it may be the basis for certain types of phenotypic cosuppression (18). It is possible that, as in nematodes as well as in plants, dsRNA may be the mediator of sequence-specific genetic silencing and cosuppression, as recently suggested by Montgomery and Fire (19). It is conceivable that in plants, animals, and trypanosomes, the pathway of dsRNA-induced RNA degradation or RNA interference (17–19) serves a

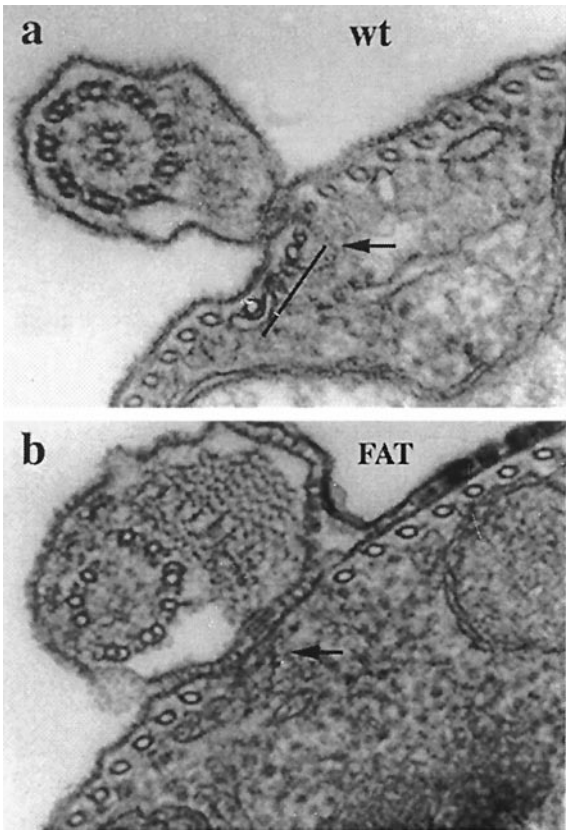

FIG. 5. Transmission electron micrographs of thin sections through the flagellum area in control (*a*) and 20-hr FAT (*b*) cells. The flagellum of control cells (wt) contains the axoneme consisting of 9 + 2 microtubules, the PFR, and a filamentous structure (arrow) that extends from the PFR into the cell body, where it interrupts the regular spacing of the cortical microtubules. Four adjacent microtubules (microtubule quartet, indicated by a bar) immediately to the left of the filamentous structure are distinct because of their association with endoplasmic reticulum cisternae and other properties discussed in the text. In at least one flagellum of FAT cells, the axoneme lacks the central microtubule pair and some of the outer doublets are missing or have an altered morphology, whereas the PFR appears normal. Also missing is the microtubule quartet and some cortical microtubules in the area where the flagellum is anchored to the cell body through the filament system (arrow). (×100,000.)

biological purpose, perhaps as a surveillance device against viruses, or in trypanosomes, as a self-regulating mechanism of gene expression. Considering the early divergence of trypanosomes from the main eukaryotic lineage, our results strongly suggest that the phenomenon of RNA interference is probably an ancient eukaryotic function.

We found that transient introduction of gene-specific dsRNAs in *T. brucei* cells resulted in selective degradation of the corresponding mRNAs. Although the decrease in the steady-state level of the various mRNAs was substantial, we always observed some residual intact mRNA even at the highest concentrations of dsRNA electroporated into trypanosomes. It is likely that this residual mRNA derives from cells that escaped electroporation because in our experiments, the efficiency of dsRNA delivery to trypanosome cells was always ≈90–95%. Thus, under our experimental conditions, RNA interference did not show 100% efficacy and was only transient. To improve our ability to use the power of RNA interference for genetic manipulation, we have recently constructed trypanosome cell lines conditionally expressing α-tubulin dsRNA from a tetracycline-inducible promoter (20). Because these cells acquire the FAT phenotype on incubation with the inducer (E.U. and E. Wirtz, unpublished data), we are now in a position to use RNA interference in a controllable fashion.

In the case of α-tubulin, our experiments show that pre-mRNA levels are not detectably affected when dsRNA is electroporated into cells. Thus, either the dsRNA does not enter the nucleus (which is unlikely because electroporation is commonly used to deliver DNA to the nucleus) or the enzyme(s) responsible for degradation of the target mRNA is not present in the nucleus or cannot act on the pre-mRNA. What could be the mechanism of dsRNA-mediated mRNA degradation? In exponentially growing trypanosomes, most mRNA molecules are associated with ribosomes and are actively translated; thus, it is likely that the mRNA is targeted for destruction while being translated. Considering that dsRNA-mediated mRNA degradation is specific, one needs to postulate that the dsRNA has to contact the target mRNA. This may occur in two different ways. The dsRNA as such may interact with the target mRNA via formation of a triple helix. This seems unlikely considering that triple-helix formation under physiological conditions may be difficult to achieve (21). The second possibility is that on entry into the cytoplasm, the dsRNA is unwound by helicases and the antisense RNA strand forms a duplex with the target mRNA. Irrespective of the type of interaction involved in recognition between the dsRNA and its target mRNA, translation of the target mRNA loaded on polyribosomes may be halted. The translational arrest may in turn accelerate degradation of the stalled mRNA. Once the molecular mechanism underlying this phenomenon is understood, it will become clear whether it is mechanistically related to genetic interference by dsRNA in *C. elegans* (17) or to RNA-mediated RNA degradation in plants (18).

From a cell biology point of view, FAT RNA-mediated destruction of α-tubulin mRNA induced a transient knockout of α-tubulin expression leading to the appearance of FAT cells with multiple nuclei and abnormal morphology. Our results showed that between 1 and 10 hr after electroporation, FAT cells progress through the cell cycle, as evidenced by their ability to duplicate and segregate the basal body, the kinetoplast, the flagellum, and the nucleus, but were unable to complete cytokinesis. When α-tubulin synthesis resumed at later times, the FAT cells carried out a new round of division of nuclei and basal bodies (Fig. 4), but again did not divide the cell body. These observations, we believe, add to our current understanding of the cell biology of trypanosomes. First, it appears that among all of the microtubule-mediated events in the trypanosome cell cycle, cytokinesis showed the highest sensitivity to alterations of the pool of newly synthesized tubulin. Second, the cells did not regain the ability to divide once cytokinesis was blocked, even when tubulin synthesis was no longer limiting. One possible interpretation of this latter finding is that FAT cells, while starving for α-tubulin, lost a cue necessary to divide the cell body and that the establishment of this cue was directly or indirectly microtubule-mediated. One of us previously has proposed (14) that the flagellar attachment zone area of the new flagellum marks the position and direction of the cleavage furrow. We think that the finding that the cytoskeletal cortex juxtaposed to the abnormal flagellum of FAT cells—namely the flagellar attachment zone and associated microtubles—was often incomplete is significant and suggests that the integrity of the cytoskeletal elements of the flagellar attachment zone is involved in establishing the path of the cleavage furrow during cytokinesis.

We thank Karl Hoffman for the scanning electron microscopy and Anna Polotsky for technical assistance. E.U. is the recipient of a Burroughs Wellcome Fund Scholar Award in Molecular Parasitology. This work was supported in part by National Institutes of Health Grant AI28798.

1. Lee, M. G. & Van der Ploeg, L. H. (1997) *Annu. Rev. Microbiol.* **51,** 463–489.
2. Agabian, N. (1990) *Cell* **61,** 1157–1160.
3. Nilsen, T. W. (1995) *Mol. Biochem. Parasitol.* **73,** 1–6.
4. Hajduk, S. L., Adler, B., Madison-Antenucci, S., McManus, M. & Sabatini, R. (1997) *Nucleic Acids Symp. Ser.* 15–18.
5. Stuart, K., Allen, T. E., Heidmann, S. & Seiwert, S. D. (1997) *Microbiol. Mol. Biol. Rev.* **61,** 105–120.
6. Alfonzo, J. D., Thiemann, O. & Simpson, L. (1997) *Nucleic Acids Res.* **25,** 3751–3759.
7. Matthews, K. R., Tschudi, C. & Ullu, E. (1994) *Genes Dev.* **8,** 491–501.
8. Sherwin, T. & Gull, K. (1989) *Cell* **57,** 211–221.
9. Kimmel, B. E., Samson, S., Wu, J., Hirschberg, R. & Yarbrough, L. R. (1985) *Gene* **35,** 237–248.
10. Schlaeppi, K., Deflorin, J. & Seebeck, T. (1989) *J. Cell Biol.* **109,** 1695–1709.
11. Muhich, M. L. & Boothroyd, J. C. (1988) *Mol. Cell. Biol.* **8,** 3837–3846.
12. McNally, K. P. & Agabian, N. (1992) *Mol. Cell. Biol.* **12,** 4844–4851.
13. Woodward, R. & Gull, K. (1990) *J. Cell Sci.* **95,** 49–57.
14. Robinson, D. R., Sherwin, T., Ploubidou, A., Byard, E. H. & Gull, K. (1995) *J. Cell Biol.* **128,** 1163–1172.
15. Woods, A., Sherwin, T., Sasse, R., MacRae, T. H., Baines, A. J. & Gull, K. (1989) *J. Cell Sci.* **93,** 491–500.
16. Scott, V., Sherwin, T. & Gull, K. (1997) *J. Cell Sci.* **110,** 157–168.
17. Fire, A., Xu, S., Montgomery, M. K., Kostas, S. A., Driver, S. E. & Mello, C. C. (1998) *Nature (London)* **391,** 806–811.
18. Metzlaff, M., O'Dell, M., Cluster, P. D. & Flavell, R. B. (1997) *Cell* **88,** 845–854.
19. Montgomery, M. K. & Fire, A. (1998) *Trends Genet.* **14,** 255–258.
20. Wirtz, E. & Clayton, C. (1995) *Science* **268,** 1179–1183.
21. Cheng, Y. K. & Pettitt, B. M. (1992) *Prog. Biophys. Mol. Biol.* **58,** 225–257.
22. De Lange, T., Berkvens, T. M., Veerman, H. J., Frasch, A. C., Barry, J. D. & Borst, P. (1984) *Nucleic Acids Res.* **12,** 4431–4443.
23. Ullu, E. & Tschudi, C. (1991) *Proc. Natl. Acad. Sci. USA* **88,** 10074–10078.